

## Constellation Pathfinder: A University Nanosatellite

C.D. Rayburn, H.E. Spence, H.E. Petschek, M. Bellino, J. Vickers, M. Murphy  
Boston University Center for Space Physics  
725 Commonwealth Avenue  
Boston, MA 02215  
(617) 353-5900  
christopher.rayburn@alum.bu.edu

N. Dennehy, D. Sargent, M. Socha  
The Charles Stark Draper Laboratory  
555 Technology Square  
Cambridge, MA 02139

**Abstract.** Constellation Pathfinder will demonstrate the feasibility of fabricating and launching three 1-kg satellites (nanosatellites) that are capable of collecting and returning quality scientific and engineering data for several months. The nanosatellite to be launched is based on one that has been under development for the past two years through the Magnetospheric Mapping Mission (MMM), a NASA New Mission Concept study. The study objective of MMM is to assess the feasibility of placing hundreds of nanosatellites equipped with magnetometers into orbits extending into the tail of the magnetosphere, thereby obtaining a much more detailed three-dimensional picture of dynamic phenomena in geospace than has been possible previously. The Constellation Pathfinder Mission (CPM) will take the first step toward such an ultimate implementation by launching similar satellites from the Shuttle. The hardware demonstration of building and flying such a satellite, or small suite of satellites, will provide a proof of principle of the satellite design that will be helpful in many scientific and strategic applications where a fleet of small satellites is required.

### Introduction

The Constellation Pathfinder Mission (CPM) is modeled from our current conceptual design for the Magnetospheric Mapping Mission (MMM). MMM will place several hundred nanosatellites weighing 1 kg into orbits with perigees at  $1.4 R_E$  and apogees that range from 5 to  $25 R_E$ . This constellation of satellites is intended to measure only magnetic field. Data will be collected over the entire orbit, stored and downloaded at perigee.<sup>1</sup>

CPM will make use of launch availability for a limited number of prototypes through the Shuttle Hitchhiker Program, sponsored jointly by the USAF and DARPA. These nanosatellite prototypes will have some adaptations from the MMM design due to differences in launch mechanisms and orbits. The magnetometer will be measuring larger, and therefore easier to measure, fields in the Earth's ionosphere; the lower altitude reduces radio frequency (RF) communication requirements as does relaxation of the required data transmission rate; and finally the natural radiation environment will be much less severe than in the MMM orbits.

The nanosatellites' basic mechanical structure is unchanged from MMM and consists of an inner core surrounded by an outer shell. The inner section consists of the batteries and satellite electronics with communication, data collection and reduction capabilities. The outer surface consists of solar cells and the support structure for the satellite. Satellite spin will maintain the orientation of both the RF antenna and the solar cells within 30 degrees of the ecliptic plane.

A three-axis fluxgate magnetometer will be able to measure magnetic fields to an accuracy of 1%. For CPM, the satellites will be in known fields over the entire orbit and the field measurement will serve largely as a check of the functioning of the magnetometer. For the high field regions ( $>10,000$  nT), this is the same as the low-altitude portion of the MMM requirement, but MMM must in addition be capable of measuring fields in the outer magnetosphere that can be as small as 1 nT. A sun sensor will be used to look radially outward and determine the spacecraft rotation phase. The sun sensor and magnetometer, used together in a known

magnetic field, will be used to determine the spin axis of the satellite. Since the spin axis changes very slowly, its orientation at a later time can be extrapolated. Given the spin axis and the phase of the spin angle we will be able to determine the satellite orientation at any time. In both missions the satellite's initial spin axis will be determined by the orientation of the mother ship from which it is released. In the MMM case, the mother ship will be the launch vehicle that achieves the desired orbit. In CPM, the three satellites will be released from a small mother ship that is released from the Shuttle.

As compared to typical satellite designs this mission is particularly stringent in terms of requiring low mass and low power. In view of the large numbers of satellites eventually involved, the design must address manufacturability – simplicity of fabrication, assembly and calibration. On the other hand, the large number of satellites also reduces the reliability requirements. Failure of a few satellites simply reduces the number of data points but it does not lead to mission failure.

This paper updates the progress of the CPM design. Specifically, preliminary results in areas including satellite design, orbital mechanics, thermal design, structural design, and attitude determination and control are discussed.

### Orbital Mechanics

The proposed launch scenario for MMM would involve placing a bus into a  $1.4 R_E$  by  $5 R_E$  orbit. This bus would carry the satellites and also a rocket motor, propulsion fuel, guidance and control equipment, and satellite release mechanisms. Acceleration would occur at perigee with a slow burn and as the perigee velocity is increasing satellites would be released individually. Thus each succeeding satellite would have a slightly higher velocity and thus apogee. The furthest orbits will have apogees at  $25 R_E$  and all satellites will share the  $1.4 R_E$  perigee. Since this scenario monotonically accelerates the bus through the various satellite orbits, it eliminates a requirement for propulsion on the individual satellites and also minimizes the propulsion fuel required.

The selection of a high perigee altitude increases the range over which the satellite is visible from a ground station and, therefore, reduces the number of ground stations required.

For the Constellation Pathfinder mission, the location and shape of the constellation is dictated by the

launch vehicle. In this case a bus of several satellites will be released from the shuttle in a 210-nm orbit with an inclination of 51.68. Included on this bus will be three nanosatellites from Boston University in addition to others university-built satellites. The decision to deploy three satellites was based on the technology demonstration goals of the mission. By releasing multiple nanosatellites, we are able to test both the satellites and the possible release mechanisms.

Using Analytical Graphics' Satellite Tool Kit version 4.03 the predicted the lifetime of the Constellation Pathfinder is 89 days (see Figure 1). This model takes into account the expected solar activity on the April 1, 2001 launch date using a 1997 model. This model was also run with solar activity 2 sigma greater than that expected at launch. In that case the satellite was found to decay in 68 days.

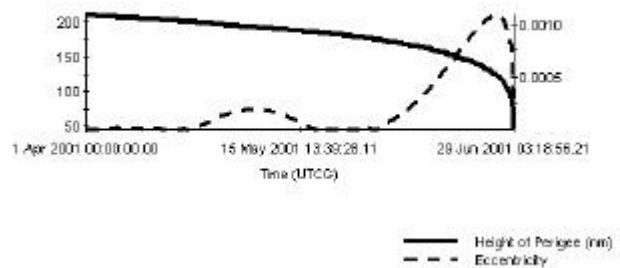


**Figure 1:** Shown is the altitude and eccentricity of the satellite as a function of time. The predicted orbit lifetime if launched on April 1, 2001 is 89 days.

### General Satellite Configuration

The general satellite configuration is shown in Figure 2. The outer hexagonal surface consists of solar cells mounted on a structural frame. The satellite electronics including batteries will be concentrated in the center. Here, radiation protection can be provided by means of a 40-mil aluminum box. MMM additionally requires the use of radiation hardened components and possibly spot shielding for particularly sensitive parts. The transmitting antenna is connected to the electronics box and is aligned with the (rotation) axis of the cylinder. Satellite spin will maintain the orientation of both antenna and solar cells to within 30 degrees of nominal.

The magnetometer will be body-mounted; its exact location will be where spacecraft magnetic fields are minimized. In the MMM implementation, this is a particularly difficult technical issue to solve and such problems will be explored in the CPM program. We hope that the magnetometer can be located within the electronics box, however, this will be subject to testing. The fact that this is a single instrument satellite that will be making measurements at a low data rate allows for the possibility of turning off some components in order to control currents during the brief periods of actual data collection. Additionally, small coils that cancel fields caused by remaining currents may be required.<sup>2</sup>

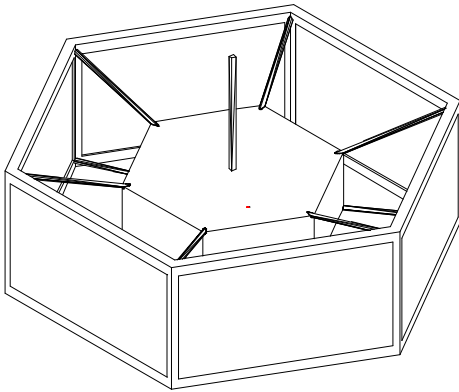


**Figure 2:** External view of satellite configuration. Circuitry will be near the center and magnetometer will be internal if adequate magnetic cleanliness can be achieved.

The power supply is being designed for one-watt average power derived from solar cells. Peak power requirements of up to five watts largely for data transmission will be available by using battery storage. Additionally some of the higher apogee MMM satellites may be eclipsed for up to 6.5 hours and battery storage must be sufficient to maintain operation during that time. This can be accomplished with the equivalent of five AA, rechargeable NiCd batteries in series. The basic electronics are designed to operate at +5 volts with a switched capacitor power inverter to provide a small amount of power at -5 volts.

The overall size of the satellite is determined predominantly by the solar cells and the average power requirement. The GaAs solar cells selected have an efficiency of 18.5%. Allowing for a 10%

degradation in power output due to radiation damage at EOM, 6 panels of 10 cm by 6 cm cells will provide over two watts of average power. This leaves margin to allow for incomplete coverage of the area due to connectors etc., the angle of incidence of sunlight not being 90° and the fact that for CPM the satellite will be eclipsed half of the time. The noted radiation degradation is consistent with 40 mils of glass over the solar cell that brings the mass of the shielded cells to 40 g.<sup>3</sup>

### Thermal Design

In order to determine the thermal design of CPM, we must consider both the requirements of CPM and of MMM. The more rigorous thermal requirements arise from MMM, but we wish to satisfy these more stringent requirements even in the CPM test flight. For apogees ranging from 5 to 25 R<sub>E</sub> in MMM, the design must consider operation both in continuous sunlight and in eclipse for up to approximately 6.5 hours.

If the satellite were a single thermal unit, then the cooling due to radiation from the solar cells during eclipse would be excessive. Since the solar area is determined by the power requirements, this cannot be decreased. In order to keep the electronics package close to 20° C it then becomes necessary to thermally isolate the electronics from the solar cells. The solar cells have a much larger temperature tolerance and can be allowed to get to very low temperatures. This isolation requires that both the struts making the mechanical structure and the electrical connections have a high thermal resistance. Additionally, the thermal balance on the electronics package must be considered.

### **Heat Conduction in Wires**

In selecting wires used to connect the solar panels to the electronics package, a voltage drop of less than 0.1 V (negligible compared to the 5V that we are using) was deemed acceptable. For a power consumption of 1 W the current is 0.2 A. #39 gage copper wire, has a resistance of 1 kΩ/1000-ft gives a per wire resistance of 0.5Ω. For acceptable voltage drop any larger diameter wire can be used.

For the #39 gage wire the heat conduction for a 140° C temperature differential would be 24 mW. Since this is small compared to power capability of 1 W, there is a margin left to allow use of somewhat larger wire that may be handled more easily.

## Heat Conduction in Structure

It is desirable to minimize the heat transfer in structural members due to the large range of temperatures seen by the solar panels. Because the heat transfer is proportional to the cross sectional area, this leads us to minimize the cross sectional area of the structural supports. In doing so we also increase the stresses experienced by the struts. The limit to the decreases in structural area must then be when the deflections approach the elastic limit of the material.

As outlined in the Structural Design section, the member area connected to the electronics box is 1.09 cm<sup>2</sup> for the sum of all the struts. The thermal conductance of the structural material EXTREN<sup>®</sup> is given as 0.178 W/m-K giving a maximum heat conduction of 167 mW. This is small compared to the 1 W of power dissipated in the satellite and is deemed acceptable.

## Electronics Package

The electronics package must remain thermally balanced when the satellite is in eclipse, when the electronics package is shadowed by the solar cells, and when it is in full sunlight. This must be done while 1 W is being dissipated on the inside.

The fact that 1 W must be radiated when in eclipse indicates that a thermal blanket surrounding the package must be sufficiently conducting to allow that heat transfer. It also requires that the blanket temperature must be high enough so that the 1 W can be radiated into space. On the other hand, when sunlit, the solar energy that is absorbed must also be radiated from the surface outside the insulation. This in turn requires a temperature rise of the outer layer and as a result also of the electronics box itself.<sup>4</sup> Present analyses indicate that this would be too large a temperature rise if a uniform insulating shield is assumed all around the box. We are presently exploring the possibility that a non-uniform heat shield would yield a smaller temperature rise and be usable.

During eclipse, the power that is lost by heat conduction through the struts and wiring could be compensated for by increasing the dissipation inside at these times. For the numbers assumed above, this would require the addition of one battery, 25 g, in order to maintain power during the maximum eclipse duration. It may be possible to do something similar

for the difference between being illuminated or shaded.

## Structural Design

The structural load is based on a 10g acceleration in all directions during launch and with an electronics box mass of 0.6 kg. Before release, each satellite will be attached to the launch vehicle at four points on the outer shell. The design criterion for the support structure is that it be able to support the weight of all components during this condition without exceeding the structural material's yield strength. It is assumed that the load of the electronics box is divided equally over the twelve connecting supports. For structural design purposes a force of 4.9 N will be applied in each direction at all of the corners.

The stringent thermal design factors led to the selection of a structural material with a low thermal conductivity. One such material is fiberglass manufactured from EXREN<sup>®</sup> - Series 635, produced by MMFG. In addition to being lightweight, this material has a low thermal and electrical conductivity, is UV resistant and is non-magnetic. More detailed specifications are shown below.

Property	Symbol	Value
Modulus of Elasticity	E	19.3 GPa
Shear Modulus	G	2.93 GPa
Poisson's Ratio	$\nu$	0.33 cm/cm
Density	$\rho$	0.065 lb/in <sup>3</sup>
Thermal Conductivity	k	0.178 W/m-K
Estimated Yield Strength		38.6 MPa

**Table 1:** Material Properties of EXTREN – Series 635 per ASTM test procedures.

Several designs were considered to fulfill the structural requirements of the nanosatellite. The most promising design consists of 12 spars connecting each corner on the outer shell to the corresponding corner on the electronics box (see Figure 2).

Each support consists of a circular rod of radius 0.17 cm corresponding to a cross sectional area of 0.0906 cm<sup>2</sup>

A finite element model of the frame was created in ANSYS version 5.5.1 in order to predict the deflection and stresses in the beam elements. Four of

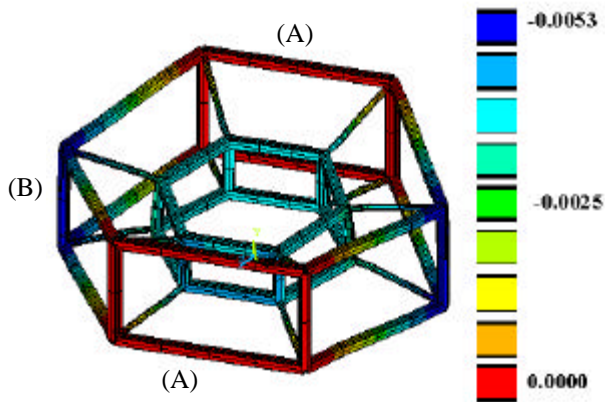


**Figure 3:** Vertical displacement under 10gs of a acceleration. The restrained corners are noted by (A) and the free corners are denoted (B). The model assumes that there are no moments at the joints. The maximum displacement in this model is 0.0053 cm at (B). All values are in centimeters.

the six outside corners are restrained and the other two are free to move. The results (Figure 3) show a maximum displacement of 0.0053 cm at both of the unrestrained outer corners. This stress associated with this displacement is well below the material's elastic limit and represents a safe displacement and stress condition.

Two other designs are also being considered for the nanosatellite. Both of these designs would reduce the deflection at the unrestrained corner. The first adds two cross braces at each corner. Note that as in the previous model there are no moments allowed at the

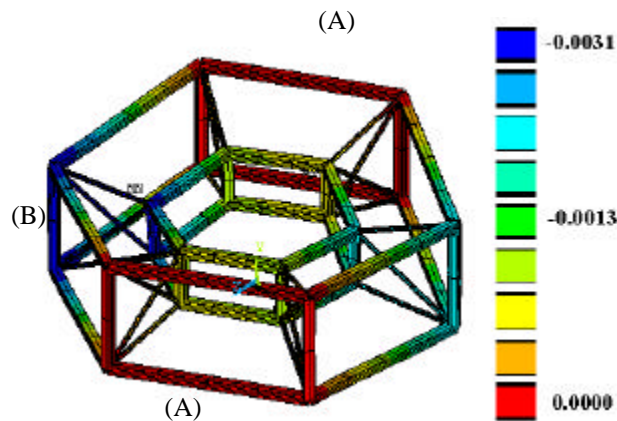


**Figure 4:** Vertical displacement under 10gs of a acceleration. The restrained corners are noted by (A) and the free corners are denoted (B). The model assumes that there are no moments at the joints. The maximum displacement in this model is 0.0031 cm at (B). All values are in centimeters.

joints.

In order to maintain the same heat transfer from the electronics during eclipse the dimension of each of the supports is reduced. Given the new dimension of the connecting spars it was found that the struts would not sustain any load in compression. While the resulting deflections were reduced by 40% (Figure 4), the manufacturing difficulty increases with this design.

Finally, all of the struts were replaced with a single shell structure. This thickness of this shell was governed by the thermal requirements and is 0.023 cm. Using this value for the thickness of the shell a finite element model was built in ANSYS, a load in each direction was then applied to each of the corners of the electronics box and the resultant displacements and stress are plotted in Figure 5. Displacements in the shell design were found to be 70% less than the original design. Again the manufacturing difficulty of such a design is high and buckling due to thermal expansion is a concern.

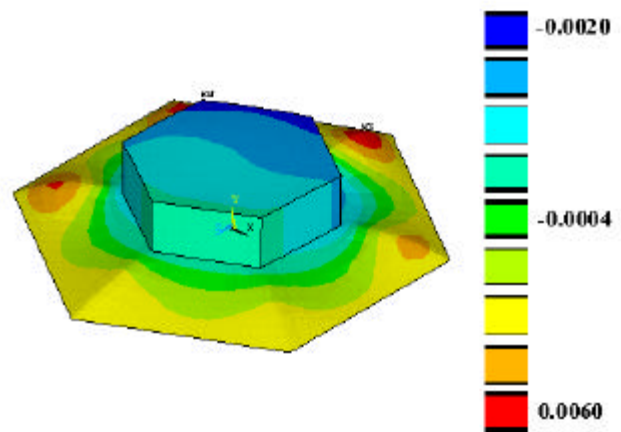


**Figure 5:** Vertical displacement under 10gs of a acceleration. In this case a load was applied to the electronics box. The maximum displacement in this model is 0.00151 cm.

Of the three designs presented to fulfill the structural requirements of the nanosatellite, we anticipate using the first design. Before the structural design is finalized two areas need further study. The selection of solar panels and their substrate needs to be completed to be sure the associated deflections will be acceptable. Also, an analysis will be completed to determine the effect of vibrations on the satellite.

## **Attitude Determination and Control**

The direction of the spin axis of the satellite will be determined using the magnetometer and sun sensor. The magnetometer will be used to define the magnetic field direction in satellite coordinates in regions where the magnetic field is well known. When this information is combined with the earth-sun line obtained from the sun sensor, spacecraft attitude can be determined. For a magnetic field direction and a spin axis having a large angle between them, this measurement would have an uncertainty corresponding roughly to the combined uncertainties in the two vectors.

For the MMM mission the magnetic field at a perigee of  $1.4R_E$  is  $\sim 10^4$  nT and about three times larger for CPM. In order to determine the orientation in the MMM case to half a degree the magnetic field must be known to better than 100 nT. While variations due to magnetospheric activity and ionospheric currents can produce disturbances up to  $10^3$  nT at high latitudes in the auroral zones, in the  $\pm 50^\circ$  latitude range the variations are below about 50 nT.<sup>5</sup> Therefore if measurements are made within this latitude range the accuracy should be sufficient

In order to achieve  $1^\circ$  angular resolution of the magnetic data, we need a sun sensor that will sense the phase angle of the satellite rotation to  $\leq 0.5^\circ$  and will accept a  $\pm 30^\circ$  tilt of the satellite relative to the ecliptic. A search of commercially available sun sensors has found sensors that achieve this angular resolution and have an appreciably wider acceptance angle. However, they have sizes that would occupy a significant fraction of our satellite volume and are therefore deemed unacceptable.

A design that would achieve our objective consists of a 2 cm by 2 cm by 2 cm box, with a front slit that is 1 cm by 0.01 cm adjacent to a 0.01 cm diameter hole at the back, followed by a photodiode. The width of the light pulse detected by the photodiode will correspond to about  $1.5^\circ$  degrees of satellite rotation and is made up of roughly equal contributions from the size of the sun, ray tracing through the slit/hole geometry and diffraction from the slit edges. The detection circuit will locate the peak of the light pulse by finding the midpoint between the two times at which the signal crosses a preset threshold. Other signals such as back scatter from the earth or moon should be lower than the solar signal by several orders of magnitude allowing for a considerable range over which the threshold can be set. The length of the slit was chosen so that essentially the same

signal will be received through the hole as long as the satellite axis is within  $\pm 30^\circ$  degrees of the perpendicular to the ecliptic.

## **Disturbance Torques**

Torques due to various sources are likely to be more significant for small satellites than they are for large satellites and need to be examined carefully. This can be seen by noting that the mass of the satellite is likely to vary as the satellite scale-size cubed while the moment of inertia varies as mass times radius squared or as the fifth power of the satellite scale size. On the other hand, torques due to drag or photon pressure will vary as the surface area multiplied by the displacement of the center of force from the center of mass or roughly as the cube of the satellite scale size. The angular acceleration, torque divided by moment of inertia, is likely to increase as the inverse square of the scale size and become a more important consideration for small satellites. A similar argument for gravity gradients results in the angular acceleration varying roughly as the inverse first power of the size scale. For magnetic torques this argument is harder to make since it depends on currents within the satellite. A number of aspects of the torque problems are discussed however additional analysis is required to complete the design.

The need for analysis of torque effects is further enhanced because our design depends on passive spin stabilization in order to minimize mass. We have quantified disturbances due to the gravity gradient, solar radiation, magnetic field, and aerodynamic drag. Owing to the low altitude Shuttle orbit, aerodynamic drag is the dominant torque for the CPM. For the MMM orbits, solar radiation pressure is dominant.

Both the gravity gradient and magnetic torques for a fixed satellite orientation are anti-symmetric in the orbit around the earth. Also since the angular momentum change during an orbit is small, the satellite orientation remains essentially fixed and these torques average to zero. Aerodynamic drag would also cancel if the atmospheric density were uniform around the orbit. However, at Shuttle altitudes there is a day night asymmetry that is more than a factor of two.

Before calculating the magnitudes of the other torques, consider the effect of the torques. Since the satellite is spinning and ideally symmetric about the spin axis there will be no torques about the spin axis and, therefore no change in the magnitude of the

angular momentum. Care must be taken to avoid the torque effect that appears on a spinning paddle wheel with black and white surfaces on opposite sides of the paddles. In other words, not only the geometry but also the reflection and absorption coefficients must be symmetric around the spin axis. Torques that can exist are from asymmetries along the spin axis and therefore are perpendicular to the spin axis.

The torques must also be perpendicular to the direction from which the radiation or the flow is coming, i.e. the drag or force vector. For a torque perpendicular to both the drag direction and the spin axis, simple geometric construction shows that the component of angular momentum parallel to the force vector will remain constant while the component perpendicular will rotate around the force vector. This is the rotation of the angular momentum vector itself, NOT the rotation about the angular momentum vector or spin axis.

The satellite will have a nutation damper either inherently due to structural dissipation or explicitly through the addition of a damping mechanism. This will be designed to damp the nutation much faster than the torques cause angular momentum changes so that nutational motion is small enough to be ignored. Since the satellite spin rate of 4 rps is much faster than the angular acceleration, a wide range of damping rates will satisfy this criterion.

### *Nature and Magnitude of Torques*

To understand the nature of the torques that can exist for aerodynamic drag at low densities and for photon pressure, we note that the two mechanisms are basically similar physically. Both may be viewed as a stream of particles moving in straight lines which when they hit the satellite surface transfer momentum by absorption, reflection or scattering. In both cases there is a small spread in directions at which the particles are moving. For the aerodynamic drag case this is due to the thermal velocities of the particles and for the photon pressure it is due to the finite size of the sun. Since it is small, we have so far neglected the spread in both cases.

It is instructive to first examine the case in which the particles are all absorbed and transfer all of their momentum to the satellite. In this case we may note that the torque is zero at any orientation for a satellite whose external shape is symmetric about every line that goes through the center of mass. This can be seen by projecting the body shape on a plane perpendicular to the direction of particle flow. For a

body with the three dimensional symmetry on every line going through the center of mass, the same symmetry will exist in the projection on the plane. Each point on the projection and its symmetric point will exert equal and opposite torques about the center of mass. Since the torque for every point is cancelled, the torque on the entire satellite will be zero. This concept is shown graphically in Figure 6.

From this idealized example it becomes evident that torques can result from asymmetry in the shape or asymmetries in the surface absorption, reflection and scattering properties. Asymmetries in shape can, within some tolerance, be avoided in the design, although this would require a second antenna, or dummy antenna, on the other side of the satellite. The larger effect is differences in the surface properties. For instance, in the above the point **Q** shown is on the face of a solar panel while **Q'** is on the back of the solar panel. Requiring equal absorption and emission coefficients at these two points may be in conflict with thermal balance requirements. For complete absorption the momentum transferred by each particle is equal in magnitude and direction to the momentum of the particle. Reflection at normal incidence from a surface causes twice the momentum transfer as absorption does. At other angles pure reflection causes a momentum transfer perpendicular to the surface that is equal to twice the component of particle momentum perpendicular to the surface. Isotropic scattering on the other hand can be viewed

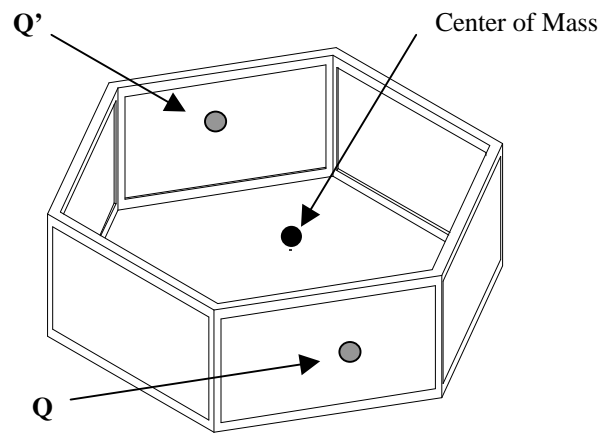


**Figure 6:** Probably the largest effect on solar radiation torques is differences in the surface properties. For instance in the diagram above the point **Q** shown is on the face of a solar panel while **Q'** is on the back side of the solar panel. Requiring equal absorption and emission coefficients at these two points may be in conflict with thermal balance requirements.

as absorption of the particle momentum plus a force perpendicular to the surface that is one half of the particle momentum.

As a descriptive form of the quantitative evaluation of the torques we may express the torque,  $t$ , as the product of a characteristic area of the satellite,  $A$ , and the force per unit area,  $P$ . This torque would occur for complete absorption of the particles multiplied by an effective displacement,  $L$ , of the center of force from the center of mass. Solving for this displacement

$$L = \frac{t}{P \cdot A} \quad (1)$$

This allows  $L$  to be taken as a descriptor for the torque when  $P$  and  $A$  are known. For solar radiation, the pressure is the incident momentum which in turn is the energy flux of solar radiation,  $1.36 \cdot 10^3 \text{ W/m}^2$  divided by the velocity of light. As a representative area we can take the cross sectional area of the satellite when viewed from a line perpendicular to the axis,  $0.0012 \text{ m}^2$ .  $P \cdot A$  then becomes  $5.44 \cdot 10^{-8} \text{ N}$ . Again, for MMM, solar radiation is the dominant torque; for CPM the dominant torque is atmospheric drag. The atmospheric drag torque depends on the satellite velocity and the atmospheric density. Using the same density as was used earlier to calculate the expected lifetime of the satellite in orbit, and a drag coefficient of 2 (corresponding to complete absorption),  $P \cdot A$  becomes  $1.9 \cdot 10^{-6} \text{ N}$ .

### **Limiting Torque Values**

For the CPM with a duration of approximately 90 days, a satellite moment of inertia of  $4.3 \cdot 10^{-2} \text{ Kg-m}^2$ , a spin rate of 4 rps, the torque in a fixed direction and specifying that the direction of the angular momentum vector changes by only  $30^\circ$ , the value of  $L$  must be 0.3 mm or less. This is very stringent when one considers that for a tilted satellite as shown in Figure 6, differences in surface material are likely to have a significant effect. We conclude that for CPM the satellite spin axis should be allowed to rotate. This is likely to create blackout periods when either the solar panels or the antenna are not oriented appropriately.

For MMM the situation is quite different because the life of the satellite is intended to be several years. The direction from which the solar radiation is coming in a fixed coordinate system varies during the course of the year i.e. the torque is in opposite directions at six

month intervals. This tends to cancel the changes in the spin axis as long as the period of rotation of the spin axis is sufficiently large compared to one year. Assuming that the torque is independent of the tilt of the satellite, an analytical analysis shows that for a ratio of periods of 3.6 or larger the spin axis has a maximum excursion of  $30^\circ$ . The nature of this motion is such that if the satellite is released with a spin axis within  $\pm 15^\circ$  range, the satellite orientation will remain within the  $\pm 30^\circ$  range which we have specified. Obtaining a this rate of rotation of the spin axis requires that  $L \leq 5 \text{ cm}$ . While we have not yet designed the shape and materials in sufficient detail to determine the  $L$  value, this is a number that can probably be achieved with sound engineering practices.

Further work in this area will involve more detailed consideration of the blackout periods in the CPM case, consideration of the fact that the torque will in fact depend on the tilt of the spin axis and detailed consideration of the torques or  $L$  values that can actually be achieved.

### **Communication**

We propose a transceiver system for both the Constellation Pathfinder and the MMM mission in which the uplink is a frequency-modulated signal and the downlink is a Viterbi-encoded data stream that modulates an RF carrier using bi-phase shift keying (BPSK). Frequency modulation of the uplink is proposed owing to the simplicity of space-based demodulation circuitry, while Viterbi encoding and BPSK modulation of the downlink enables an efficient transfer of data with a minimum of transmitted power. We have designed the transceiver using commercial RF microelectronic parts which, owing to the demands of the cellular telecommunications market, are designed for low-power operation using miniaturized packaging techniques. The basic design for both CPM and MMM are similar, though we have designed for an RF carrier in the 400 MHz band for CPM, while we anticipate an S-band RF carrier for MMM.

Initially we considered a downlink-only communication system for the MMM constellation of nanosatellites. The plan was for each nanosatellite to initiate a downlink when it crossed through a specified magnetic field shell near perigee. Using this scheme, an automated ground station would anticipate where in the sky each nanosatellite would begin transmission such that it could position its antenna to receive any transmitted data. However,



owing to the inability of a ground station to point several places at once, this scheme became increasingly difficult to implement as the number of nanosatellites in the MMM constellation grew. A better scheme, and one that greatly eases ground station demands, involves commanding each nanosatellite using an RF uplink, and scheduling the data downlinks. As a result, we have implemented a transceiver on each nanosatellite.

The earth-satellite uplink is not critical since the ground station can use a high-power transmitter. For the downlink, however, our desire to build a minimal-mass nanosatellite limits our choices in RF parts to the miniature low-power parts used in commercial cellular phones. Within that market, several RF components exist that can generate 1 Watt of RF power from a 5-volt power rail, both near 400 MHz and in the S band.

Because BPSK modulation is a constant-amplitude modulation scheme, efficient class-C amplifiers generate this RF power with, typically, 35% efficiency. As a result, a complete 1-Watt RF transmitter can be built that requires only 5 Watts of input power; the small duty cycle of the RF transmissions limits the impact of this large temporary power draw.

For CPM, the maximum link range is  $0.33 R_E$  while for MMM, the maximum link range is  $1 R_E$ . We have baselined a quarter-wave antenna for both missions, which has an RF transmission gain perpendicular to the antenna of 2 dBi. For purposes of our link equation, we assume no antenna gain, as the dipole will not, in general, be perpendicular to the RF link. Taking into consideration the nanosatellite transmission power, the path loss, atmospheric absorption, cable losses, ground station antenna gain, and receiver noise, an RF link can be maintained at a 62.5 kHz data rate. This assumes, in the case of the Constellation Pathfinder, a modest Yagi antenna, and in the case of MMM, a 2-meter dish antenna. These estimates include several dB of link margin, and are calculated for bit error rates less than  $10^{-6}$ .

### Conclusions

A Constellation Pathfinder Mission has been presented which will provide proof of principle for a larger constellation of magnetometry nanosatellites. Though differences do exist, the nanosatellite design is essentially the same as that presented for the Magnetospheric Mapping Mission. Both missions are feasible within the 1 W and 1 kg limits that

should allow for the launching of hundreds of satellites to obtain 3D magnetic field pictures in the magnetospheric tail in the range of 5-25  $R_E$ .

### Acknowledgements

This work was supported by a NASA Space Physics New Mission Concepts Program grant, NAG5-3748, and by a US Air Force AFOSR grant, F49620-99-1-0249.

### References

1. H.E. Petschek, C.D. Rayburn, R. Sheldon, J. Vickers, M. Bellino, G. Bevis, H.E. Spence. "The Kilo-Satellite Constellation Concept" *Science Closure and Enabling Technologies for Constellation Class Missions*, University of California at Berkeley Press and NASA/GSFC, February, 1999.
2. Mario Acuna and Brian Anderson private communication, 1999.
3. Ray, K.P., E.G. Mullen, and T.M. Trumble, Results from the High Efficiency Solar Panel Experiment Flown of CRRES, IEEE Transaction on Nuclear Science, Vol. 40, No. 6, pp. 1505, 1993.
4. Gilmore, David G., ed., Satellite Thermal Control Handbook, The Aerospace Corporation Press, El Segundo, CA, 1999
5. Langel, Robert et al, MAGSAT Preliminary Results, *Geophys. Res. Letters* **9**, April 1982, 239-376.